PHYSICAL REVIEW D VOLUME 43, NUMBER 11 1 JUNE 1991

ARTICLES

Inclusive production of the charmed baryon Λ_c^+ from e^+e^- annihilations at $\sqrt{s} = 10.55$ GeV

P. Avery,[a] D. Besson,[a] L. Garren,[a] J. Yelton,[a] K. Kinoshita,[b] F. M. Pipkin,[b] M. Procario,[b] Richard Wilson,[b] J. Wolinski,[b] D. Xiao,[b] Y. Zhu,[b] R. Ammar,[c] P. Baringer,[c] D. Coppage,[c] P. Haas,[c] N. Kwak,[c] Ha Lam,[c] S. Ro,[c] Y. Kubota,[d] J. K. Nelson,[d] D. Perticone,[d] R. Poling,[d] R. Fulton,[e] T. Jensen,[e] D. R. Johnson,[e] H. Kagan,[e] R. Kass,[e] F. Morrow,[e] J. Whitmore,[e] P. Wilson,[e] D. Bortoletto,[f] W.-Y. Chen,[f] J. Dominick,[f] R. L. McIlwain,[f] D. H. Miller,[f] C. R. Ng,[f] S. F. Schaffner,[f] E. I. Shibata,[f] I. P. J. Shipsey,[f] W.-M. Yao,[f] K. Sparks,[g] E. H. Thorndike,[g] C.-H. Wang,[g] M. S. Alam,[h] I. J. Kim,[h] W. C. Li,[h] X. C. Lou,[h] V. Romero,[h] C. R. Sun,[h] P.-N. Wang,[h] M. M. Zoeller,[h] M. Goldberg,[i] T. Haupt,[i] N. Horwitz,[i] V. Jain,[i] M. D. Mestayer,[i] G. C. Moneti,[i] Y. Rozen,[i] P. Rubin,[i] V. Sharma,[i] T. Skwarnicki,[i] M. Thulasidas,[i] G. Zhu,[i] S. E. Csorna,[j] T. Letson,[j] J. Alexander,[k] M. Artuso,[k] C. Bebek,[k] K. Berkelman,[k] T. Browder,[k] D. G. Cassel,[k] E. Cheu,[k] D. M. Coffman,[k] G. Crawford,[k] J. W. DeWire,[k] P. S. Drell,[k] R. Ehrlich,[k] R. S. Galik,[k] B. Gittelman,[k] S. W. Gray,[k] A. M. Halling,[k] D. L. Hartill,[k] B. K. Heltsley,[k] J. Kandaswamy,[k] N. Katayama,[k] D. L. Kreinick,[k] J. D. Lewis,[k] G. S. Ludwig,[k] N. B. Mistry,[k] J. Mueller,[k] S. Nandi,[k] E. Nordberg,[k] C. O'Grady,[k] D. Peterson,[k] M. Pisharody,[k] D. Riley,[k] M. Sapper,[k] M. Selen,[k] A. Silverman,[k] S. Stone,[k] H. Worden,[k] M. Worris,[k] and A. J. Sadoff[l]

(CLEO Collaboration)

[a]*University of Florida, Gainesville, Florida 32611*
[b]*Harvard University, Cambridge, Massachusetts 02138*
[c]*University of Kansas, Lawrence, Kansas 66045*
[d]*University of Minnesota, Minneapolis, Minnesota 55455*
[e]*Ohio State University, Columbus, Ohio 43210*
[f]*Purdue University, West Lafayette, Indiana 47907*
[g]*University of Rochester, Rochester, New York 14627*
[h]*State University of New York at Albany, Albany, New York 12222*
[i]*Syracuse University, Syracuse, New York 13244*
[j]*Vanderbilt University, Nashville, Tennessee 37235*
[k]*Cornell University, Ithaca, New York 14853*
[l]*Ithaca College, Ithaca, New York 14850*

(Received 27 August 1990)

We report results on inclusive production of the charmed baryon Λ_c^+ from e^+e^- annihilations at $\sqrt{s} = 10.5$ GeV. Measurements are presented of the inclusive cross section times branching fraction for the continuum production of Λ_c^+ as observed in six different decay modes, and of a new, improved value of the Λ_c^+ mass. The inclusive cross section times the branching fraction into $pK^-\pi^+$ is measured to be $10.0\pm1.5\pm1.5$ pb summed over all x_p. The branching fractions of Λ_c^+ into $p\bar{K}^0$, $p\bar{K}^0\pi^+\pi^-$, $\Lambda\pi^+$, $\Lambda\pi^+\pi^-\pi^+$, and $\Xi^-K^+\pi^+$ relative to that into $pK^-\pi^+$ are measured to be $0.44\pm0.07\pm0.05$, $0.43\pm0.12\pm0.04$, $0.18\pm0.03\pm0.03$, $0.65\pm0.11\pm0.12$, and $0.15\pm0.04\pm0.03$, respectively. The Λ_c^+ mass is measured to be $2284.7\pm0.6\pm0.7$ MeV/c^2. The measured momentum distributions for continuum production of Λ_c^+ are compared to analytical fragmentation functions and to other measurements.

I. INTRODUCTION

The first observation of Λ_c^+ production in e^+e^- annihilations was reported by the Mark II Collaboration[1] in 1979 in the decay mode $pK^-\pi^+$ at center-of-mass energies near 5 GeV. More recently, both CLEO[2] and ARGUS[3,4] Collaborations have reported the production of Λ_c^+ in e^+e^- collisions at center-of-mass energies around 10.55 GeV in several decay modes. The E691[5] Collaboration has also reported Λ_c^+ production from the Tagged Photon Spectrometer at Fermilab. However, the scarcity of data on charmed baryons is in contrast with the relatively large amount of data on charmed-meson production and decay. While the sum of the measured branching fractions for the charmed mesons D^0 and D^+ is nearly 100%, there are no direct measurements of the Λ_c^+ decay branching fractions. Fragmentation distributions for D^{*+}, D^0, D^+, and D_s^+ from charm jets have

now been measured by various experiments at the SLAC storage ring PEP,[6] at the DESY storage rings PETRA[7] and DORIS[8] and at the Cornell Electron Storage Ring.[9] However, there are very limited measurements on the fragmentation distributions of charmed baryons. Further, the probability that the c quark fragments into charmed baryons relative to the probability that it fragments into charmed mesons has not yet been measured directly. The study of charmed-baryon decays can also shed light on the roles of spectator, exchange and annihilation diagrams and on the extent of color mixing in charm decays.

In this paper we present substantially improved measurements of $B\sigma$, the inclusive Λ_c^+ production cross section in e^+e^- annihilations times branching fraction, as observed in six different decay modes. The charge-conjugate modes are implied in each case. The decay modes observed are presented below:

$$\Lambda_c^+ \to pK^-\pi^+ \quad (1a)$$

$$\to p\bar{K}^0 \quad (1b)$$

$$\to p\bar{K}^0\pi^+\pi^- \quad (1c)$$

$$\to \Lambda\pi^+ \quad (1d)$$

$$\to \Lambda\pi^+\pi^-\pi^+ \quad (1e)$$

$$\to \Xi^-K^+\pi^+ \,. \quad (1f)$$

In Figs. 1(a)–1(f), we show some samples of the decay diagrams for these modes in the spectator model, where the decay is primarily determined by the Cabibbo-allowed coupling of the c quark to an s quark and a virtual W^+.

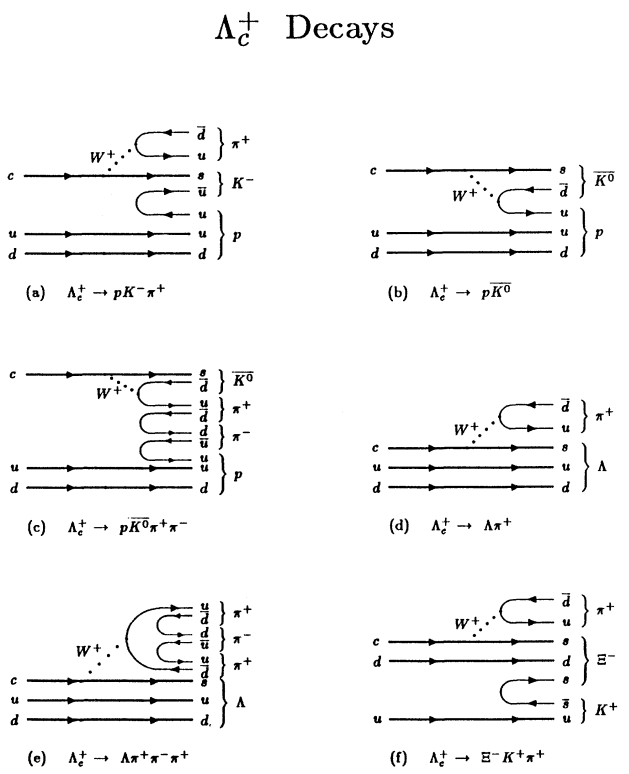

FIG. 1. Feynman decay diagrams for Λ_c^+ in the decay modes $\Lambda\pi^+$, $p\bar{K}^0$, $\Lambda\pi^+\pi^-\pi^+$, $p\bar{K}^0\pi^+\pi^-$, $pK^-\pi^+$, and $\Xi^-K^+\pi^+$.

In Sec. II, short descriptions of the detector and of the event selection procedures are given. The details of the analysis procedure are presented in Sec. III. In Sec. IV, we present the differential production cross sections with respect to the fragmentation variables x_p and x^+.[10] Here $x_p = p/p_{\max}$ and $x^+ = (E+p)/(E_{\max}+p_{\max})$. E and p are the energy and momentum of the Λ_c^+ while $E_{\max} = E_{\text{beam}}$ and $p_{\max} = (E_{\text{beam}}^2 - m_{\Lambda_c^+}^2)^{1/2}$. In Sec. V, the results of fits to different analytical fragmentation functions are presented. Section VI contains the final results of the measurements of the inclusive Λ_c^+ cross sections and the relative and absolute branching fractions. Section VII contains the conclusions.

II. SELECTION OF EVENTS AND DESCRIPTION OF THE DETECTOR

The data sample used in this study was collected with the upgraded CLEO detector at the Cornell Electron Storage Ring (CESR). It consists of 212 pb^{-1} at the $\Upsilon(4S)$ resonance ($\sqrt{s} = 10.58$ GeV) and 101 pb^{-1} at energies just below the $\Upsilon(4S)$ ($\langle\sqrt{s}\rangle = 10.52$ GeV, commonly referred to as the continuum) and 117 pb^{-1} at the $\Upsilon(5S)$ energy ($\sqrt{s} = 10.87$ GeV). The hadronic event selection criteria and the CLEO detector are described in detail elsewhere[11] and will thus be described only briefly here.

We accept hadronic events if they satisfy the following criteria: The primary vertex must lie within 5 cm of the center of the interaction region along the beam line and within 2 cm transverse to the beam line. There should be three or more charged tracks reconstructed in the drift chamber. The total visible energy should be at least 30% of the center-of-mass energy. After applying the above cuts, we have a little less than 2×10^6 hadronic events in the total data sample, of which 240 000 are $\Upsilon(4S)\to B\bar{B}$ and 35 000 are $\Upsilon(5S)\to B\bar{B}$ events.

Here we will briefly describe the recent modifications to the central tracking system. Charged-particle tracking is done inside a superconducting solenoid of radius 1.0 m which produces a 1.0-T magnetic field. Three nested cylindrical drift chambers measure momenta and specific ionization of charged particles. The innermost part of the tracking system is a three-layer straw tube vertex detector which gives a position accuracy of 70 μm in the r-ϕ plane. The middle ten-layer vertex chamber measures the position with an accuracy of 90 μm in the r-ϕ plane. The main drift-chamber system consists of 51 layers, eleven of which are strung in stereo angles of 1.9° to 3.5° to the z axis. The system has achieved a position accuracy of 110 μm and dE/dx ionization resolution of 6.5%. Measurements of the track coordinates along the beam direction (z) are achieved using stereo layers and cathode strips in the middle vertex detector and the main drift chamber. This system achieves a momentum resolution given by $(\delta p/p)^2 = (0.23\%p)^2 + (0.7\%)^2$, where p is measured in GeV/c.

III. DESCRIPTION OF ANALYSIS PROCEDURE

A. Particle identification

At the $\Upsilon(4S)$ and $\Upsilon(5S)$ energies, charmed baryons are produced from the decay of B mesons and also from e^+e^- nonresonant annihilations into $c\bar{c}$ jets. The Λ_c^+'s produced from B-meson decays are kinematically limited to $x_p < 0.5$ ($x^+ < 0.55$). In this analysis we are interested only in Λ_c^+'s produced from e^+e^- annihilations to $c\bar{c}$ pairs. For the part of the spectrum with $x_p > 0.5$ ($x^+ > 0.55$), we use the full data sample (430 pb^{-1}) consisting of the continuum $\Upsilon(4S)$ and $\Upsilon(5S)$ contributions. To measure the momentum spectrum with $x_p < 0.5$ ($x^+ < 0.55$), we use only the continuum data sample below the $\Upsilon(4S)$ (101 pb^{-1}), which is below threshold for B-meson production.

The momenta of all charged tracks as measured in the drift chambers are corrected for ionization loss in the material before the tracking chamber. Pions, kaons and protons with momenta below 0.05, 0.2, and 0.3 GeV/c, respectively, either range out in the beam pipe or are very poorly measured and hence not used in the analysis. Only measurements of the ionization losses in the 51 layer drift chamber are used for particle identification. A track is defined to be consistent with a specific mass hypothesis (pion, kaon or proton) if its measured dE/dx is within 2 standard deviations (2σ) of the expected value for that hypothesis. Corresponding to these criteria, the particle-identification efficiency for tracks reconstructed in the drift chamber is about 95% and nearly independent of particle momenta. However, there is little separation between a pion and a kaon (proton) at high momentum beyond about 0.7 GeV/c (1.1 GeV/c). A track is loosely (positively) identified as a kaon or a proton if its measured dE/dx is consistent with the corresponding hypothesis and at the same time it is 1σ (2σ) away from the pion hypothesis. For example, the proton identification efficiency corresponding to the loose (positive) criteria varies from 90% (90%) below 1.0 GeV/c to 60% (25%) at 1.5 GeV/c. For the loose (positive) identification criteria, the probability that a pion will fake a proton is negligible at momenta below 1.0 GeV/c and remains constant at about 30% (5%) for higher momenta. The actual choice of the particle-identification criteria depends on the decay mode being considered and the nature of the random background with which one is dealing. The particle-identification efficiencies are found using independently identified samples of pions from the decay $K_S^0 \to \pi^+\pi^-$, kaons from the decay chain $D^{*+} \to D^0\pi^+$, $D^0 \to K^-\pi^+$ and protons from $\Lambda \to p\pi^-$. The errors in the kaon-identification efficiencies are about 10% (15%) of the efficiency values for the loose (positive) identification criteria. The corresponding errors for the proton-identification efficiencies are 5% (10%) of the efficiency values. This uncertainty is included in calculating the systematic errors.

K^0's are detected as K_S^0's that decay to $\pi^+\pi^-$ and Λ's are identified through their decay to $p\pi^-$. Both are identified by requiring secondary vertices separated from the primary vertex. A secondary vertex is reconstructed from a pair of oppositely charged tracks such that the radial distance from the intersection point of the pairs from the primary vertex is greater than 1 mm. The pair is identified as a K_S^0 (Λ) candidate if the invariant mass of the pair when interpreted as $\pi^+\pi^-$ ($p\pi^-$) is within 12 (6) MeV/c^2 of the K_S^0 (Λ) mass, which corresponds to a $\pm 3\sigma$ mass cut based on fits to the respective invariant-mass distributions with a Gaussian function. K_S^0 and Λ candidates that are ambiguous with each other are not used. This results in a loss of about 5% for Λ's and less than

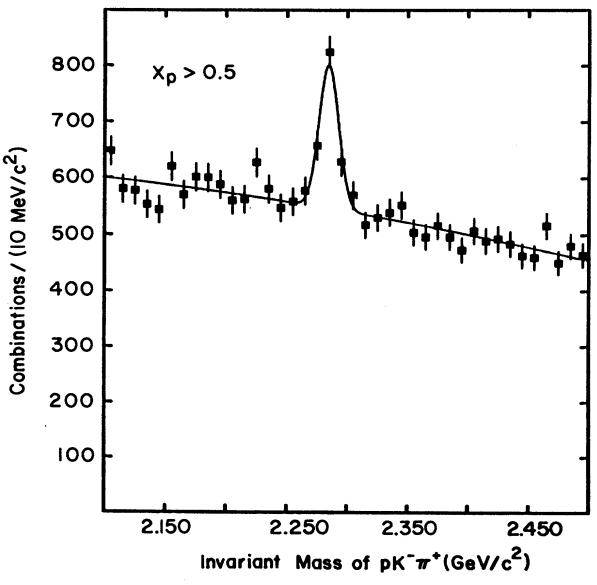

FIG. 2. $pK^-\pi^+$ invariant-mass distributions for $x_p > 0.5$.

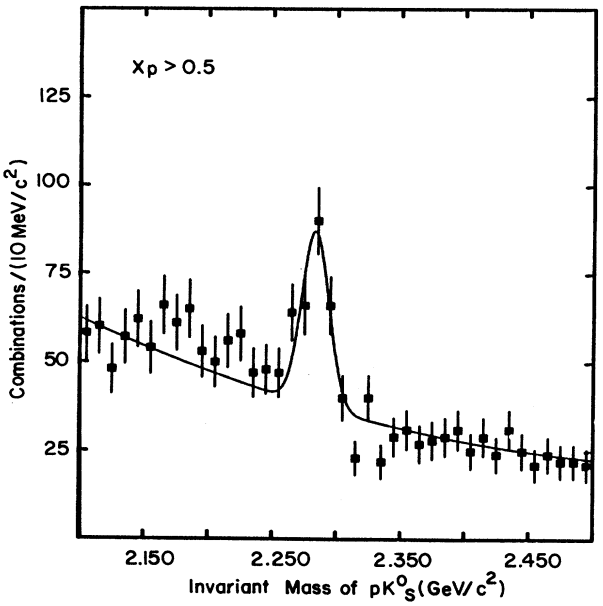

FIG. 3. $p\bar{K}^0$ invariant-mass distributions for $x_p > 0.5$.

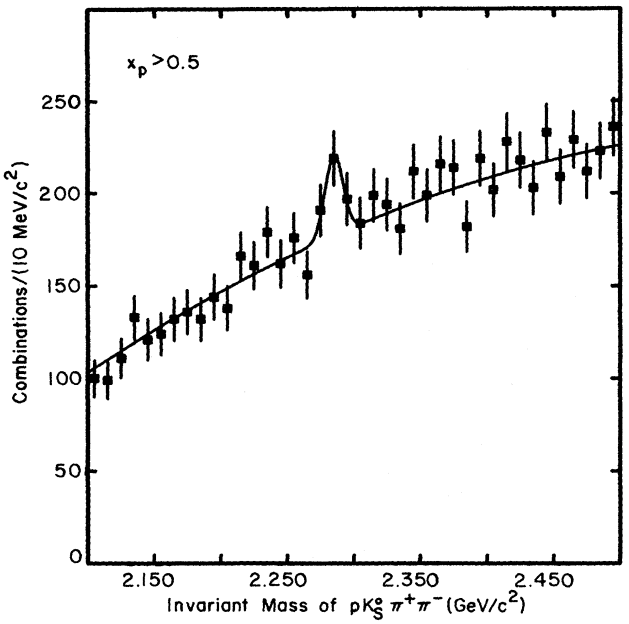

FIG. 4. $p\bar{K}^0\pi^-\pi^+$ invariant-mass distributions for $x_p > 0.5$.

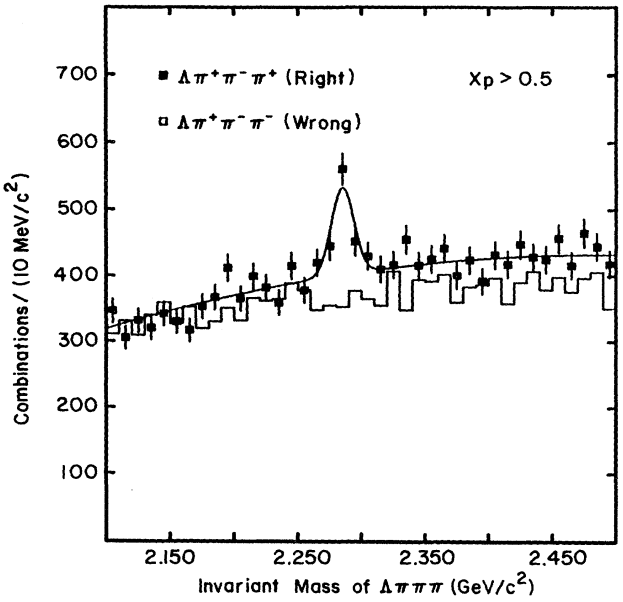

FIG. 6. $\Lambda\pi^+\pi^-\pi^+$ and $\bar{\Lambda}\pi^+\pi^-\pi^-$ invariant-mass distributions for $x_p > 0.5$.

2% for K^0_S's. The reconstruction efficiency for $K^0_S \to \pi^+\pi^-$ ($\Lambda \to p\pi^-$) below 0.2 (0.3) GeV/c is negligible and is 45% (36%) for momentum above 1.0 GeV/c, as found using a Monte Carlo simulation of the detector.

Ξ^- candidates are identified through their decay to $\Lambda\pi^-$. Combinations are made of each Λ candidate with an additional negatively charged track in the event assuming it to be a π^-. The point of intersection of the two is required to be at least 4 mm away radially from the beam line and closer to it than the Λ decay vertex. The mean distance of Ξ^- from the primary vertex is about 6 cm and the corresponding distance for Λ candidates is about 10 cm. Ξ^- candidates are selected as those combinations with a reconstructed invariant mass within 5 MeV/c^2 of the fitted Ξ^- mass (1321.5 MeV/c^2).

B. Specific decay modes

In each decay mode of the Λ_c^+ discussed below, the invariant-mass distribution is fitted to the sum of a

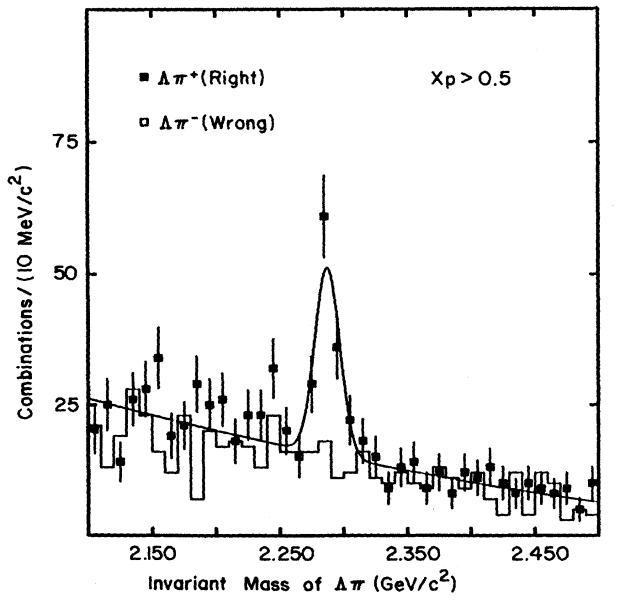

FIG. 5. $\Lambda\pi^+$ and $\bar{\Lambda}\pi^+$ invariant-mass distributions for $x_p > 0.5$.

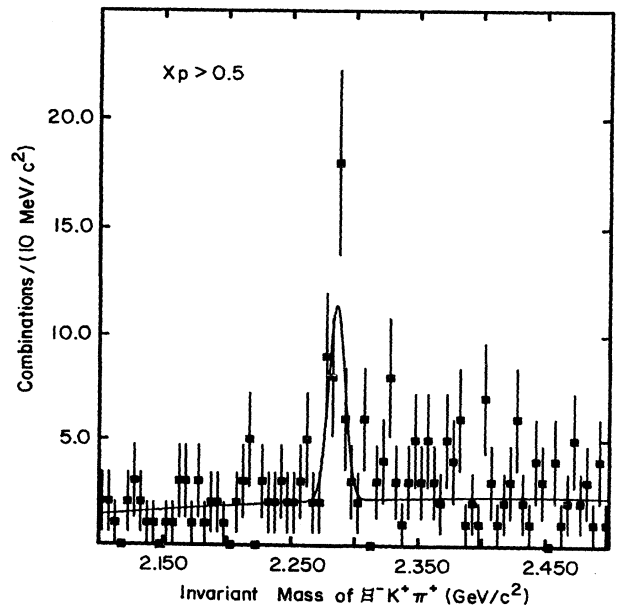

FIG. 7. $\Xi^-K^+\pi^+$ invariant-mass distributions for $x_p > 0.5$.

TABLE I. Results of fits to the mass distributions in Figs. 2–7.

Decay mode	Fitted mass (MeVc^2)	Fitted width (MeV/c^2)	Monte Carlo width (MeV/c^2)	Signal-area candidates
$pK^-\pi^+$	2284.5±0.9	17±2	19±0.4	512±50
$p\bar{K}^0$	2282.4±1.7	27±4	25±0.7	133±17
$p\bar{K}^0\pi^-\pi^+$	2283.8±3.0	16±6	16±0.9	83±23
$\Lambda\pi^+$	2287.6±1.6	17±3	23±0.8	87±12
$\Lambda\pi^+\pi^-\pi^+$	2284.2±1.7	15±2	21±1.1	289±41
$\Xi^-K^+\pi^+$	2285.5±1.5	12±3	15±0.8	30±7
	Weighted mass=2284.7±0.6±0.7 MeV/c^2			
	Mass [Particle Data Group (Ref. 12)]=2285.2±1.2 MeV/c^2			

Gaussian function and a low-order polynomial background with signal width [full width at half maximum (FWHM)] fixed at the value predicted by Monte Carlo simulation. In each case we show the invariant-mass distribution for $x_p > 0.5$; we do not show the corresponding distribution for $x_p < 0.5$ since the signal has limited statistical significance in this range of x_p.

1. $\Lambda_c^+ \to pK^-\pi^+$

In Fig. 2, we show the invariant-mass distribution for $pK^-\pi^+$ combinations with $x_p > 0.5$; we require both kaon and proton candidates to be loosely identified. For combinations with $x_p < 0.5$, since the combinatorial background is higher, the kaon candidate is loosely identified while the proton candidate is positively identified. All tracks with momenta greater than 0.3 GeV/c are used as pions. The pion momentum cut reduces the background level significantly.

2. $\Lambda_c^+ \to p\bar{K}^0$

In this mode and $p\bar{K}^0\pi^+\pi^-$ mode discussed below, $\bar{K}^0$'s are detected through K_S^0's. For combinations of pK_S^0 with $x_p > 0.5$, loose identification for protons is required. We show the corresponding invariant-mass distribution in Fig. 3. Since the combinatorial background is higher for combinations with $x_p < 0.5$, we require that the protons be positively identified.

3. $\Lambda_c^+ \to p\bar{K}^0\pi^+\pi^-$

This decay mode is dominated by a large combinatorial background and the observed signal is statistically weak. We require the impact parameter of the two pions from K_S^0's decays be greater than 1 mm. Also, we require that the proton candidates be loosely identified for invariant-mass combinations of $pK_S^0\pi^+\pi^-$ with $x_p > 0.5$ as shown in Fig. 4, and be positively identified for combinations with $x_p < 0.5$.

4. $\Lambda_c^+ \to \Lambda\pi^+$

To reduce the combinatorial background, we require that the cosine of the angle between pion and Λ_c^+ direction in the Λ_c^+ rest frame be greater than -0.7, reducing the background level by a factor of 2. The selection criteria are the same for $x_p < 0.5$ and $x_p > 0.5$. Figure 5 shows the invariant-mass distribution for $\Lambda\pi^+$ combinations with $x_p > 0.5$. The mass resolution in this decay mode is somewhat worse since the pions are relatively fast. A check on the validity of the signal is to look at the wrong strangeness and charge $\bar{\Lambda}\pi^+$ combinations. The mass distribution of $\bar{\Lambda}\pi^+$ combinations with the same selection cuts as those used for the $\Lambda\pi^+$ distribution, as displayed in Fig. 5, shows no enhancement in the region of the Λ_c^+ mass. While calculating the Monte Carlo reconstruction efficiencies for both the $\Lambda\pi^+$ and $\Lambda\pi^+\pi^-\pi^+$ mode, we assume uniform angular distribution for the Λ.

TABLE II. Inclusive production of Λ_c^+ in the decay mode $pK^-\pi^+$.

x_p	Efficiency	Yield	Corrected yield	$B(d\sigma/dx_p)$ (pb)
0.0–0.2	0.217±0.014	0±10	0±46	0±2
0.2–0.3	0.205±0.009	8±13	39±63	4±6
0.3–0.4	0.175±0.008	7±11	40±63	4±6
0.4–0.5	0.133±0.007	27±10	203±76	20±8
0.5–0.6	0.168±0.007	180±32	1071±196	25±5
0.6–0.7	0.164±0.008	186±27	1134±174	26±4
0.7–0.8	0.163±0.010	112±21	683±135	16±3
0.8–0.9	0.155±0.014	34±15	219±99	5±2
0.9–1.0	0.146±0.026	0±7	0±48	0±1
0.5–1.0		512±50	3107±315	

TABLE III. Inclusive production of Λ_c^+ in the decay mode $p\bar{K}^0$.

x_p	Efficiency	Yield	Corrected yield	$B(d\sigma/dx_p)$ (pb)
0.0–0.2	0.140±0.009	6±7	43±50	2±2
0.2–0.3	0.109±0.006	11±5	101±46	10±5
0.3–0.4	0.086±0.005	7±4	81±47	8±5
0.4–0.5	0.071±0.005	2±3	28±42	3±4
0.5–0.6	0.102±0.005	38±10	373±100	9±2
0.6–0.7	0.097±0.006	53±10	546±109	13±3
0.7–0.8	0.093±0.007	36±8	387±91	9±2
0.8–0.9	0.088±0.015	6±5	68±58	2±1
0.9–1.0	0.085±0.037	0±3	0±35	0±1
0.5–1.0		133±17	1374±186	

5. $\Lambda_c^+ \to \Lambda\pi^+\pi^-\pi^+$

Figure 6 shows the invariant-mass distribution for all $\Lambda\pi^+\pi^-\pi^+$ combinations with $x_p > 0.5$ with no other selection criteria applied. The mass distribution for the wrong strangeness and charge $\bar{\Lambda}\pi^+\pi^-\pi^+$ combinations, also displayed in Fig. 6, shows no enhancement in the region of the Λ_c^+ mass. To reduce the combinatoric background for $x_p < 0.5$ region, we require that the cosine of the angle between each of the three pions and the Λ_c^+ direction in the Λ_c^+ rest frame be greater than -0.9.

6. $\Lambda_c^+ \to \Xi^- K^+\pi^+$

For this decay mode, $\Xi^- K^+\pi^+$ combinations are formed from Ξ^- candidates together with a positively charged track which satisfied the kaon consistency criteria and another positively charged track which is assumed to be a π^+. Figure 7 shows the invariant-mass distribution for $\Xi^- K^+\pi^+$ combinations with $x_p > 0.5$.

C. Effect of pions and kaons faking protons

There is the possibility that the signals in the first three decay modes, $pK^-\pi^+$, $p\bar{K}^0$, and $p\bar{K}^0\pi^-\pi^+$, may receive contributions from D^+ decaying into $K^-\pi^+\pi^+$, $\bar{K}^0\pi^+$, and $\bar{K}^0\pi^+\pi^-\pi^+$, respectively, due to pions faking protons. We refer to such contributions as reflections. Reflections could also be present from D_s^+ decaying into $K^-K^+\pi^+$, $\bar{K}^0K^+$, and $\bar{K}^0K^+\pi^-\pi^+$, respectively, due to kaons faking protons. We have ruled out these possibilities in several ways. The most direct method used is to take the combinations in the region of the Λ_c^+ mass and to plot them as the corresponding reflections from either the D^+ or the D_s^+ by redefining the mass of the relevant particle in the combination. The same procedure is then repeated using combinations in the sidebands on either side of the signal. Comparing the size of the reflection from the signal region with that from the sidebands, we estimate that less than 5% of the observed Λ_c^+ signal in any decay mode could come from D^+ or D_s^+ reflections.

D. Summary of the mass distribution plots

The results of fits to the signals in all Λ_c^+ decay modes with Monte Carlo–predicted widths are presented in Table I. The fitted widths are consistent with the Monte Carlo–predicted values in all cases, except for the $\Lambda\pi^+$ and $\Lambda\pi^+\pi^-\pi^+$ distributions in which cases the Monte Carlo simulation overestimates the full widths. The areas of the signals using the predicted Monte Carlo widths, as reported in the table, are consistent with the results obtained using the variable widths and differ at most by 10%, which is added to our estimate of the systematic errors. The weighted average of the fitted masses is 2284.7±0.6±0.7 MeV/c^2, which may be restated as 2284.7±0.9 MeV/c^2 if we add the statistical and systematic errors in quadrature. The systematic error depends on the accuracy of the energy-loss correction applied to the kaon and proton tracks. Our measurement is

TABLE IV. Inclusive production of Λ_c^+ in the decay mode $p\bar{K}^0\pi^+\pi^-$.

x_p	Efficiency	Yield	Corrected yield	$B(d\sigma/dx_p)$ (pb)
0.0–0.2	0.045±0.011	0±8	0±178	0±9
0.2–0.3	0.056±0.009	13±10	232±182	23±18
0.3–0.4	0.063±0.007	24±9	381±149	38±15
0.4–0.5	0.056±0.007	5±6	89±108	9±11
0.5–0.6	0.074±0.007	18±15	243±204	6±5
0.6–0.7	0.065±0.007	31±13	477±207	11±5
0.7–0.8	0.058±0.009	18±9	310±161	7±4
0.8–0.9	0.054±0.011	15±7	278±141	6±3
0.9–1.0	0.050±0.016	1±3	20±60	1±1
0.5–1.0		83±23	1328±366	

TABLE V. Inclusive production of Λ_c^+ in the decay mode $\Lambda\pi^+$.

x_p	Efficiency	Yield	Corrected yield	$B(d\sigma/dx_p)$ (pb)
0.0–0.2	0.182±0.019	6±8	33±44	2±2
0.2–0.3	0.175±0.014	7±7	40±40	4±4
0.3–0.4	0.162±0.012	9±6	56±37	6±4
0.4–0.5	0.180±0.013	2±5	11±28	1±3
0.5–0.6	0.161±0.012	23±7	143±45	3±1
0.6–0.7	0.160±0.013	35±7	219±47	5±1
0.7–0.8	0.159±0.017	18±5	113±34	3±1
0.8–0.9	0.155±0.019	10±4	65±27	2±1
0.9–1.0	0.150±0.039	0±4	0±27	0±1
0.5–1.0		86±12	540±83	

an improvement over the Particle Data Group value[12] of 2285.2±1.2 MeV/c^2, which includes the systematic error, and is the weighted average of many different experiments.

IV. THE FRAGMENTATION DISTRIBUTIONS

In order to study the fragmentation of the charm quark into the charmed baryon Λ_c^+, the momentum spectra of the Λ_c^+'s as observed in the various decay modes are studied in terms of the fragmentation variable x_p and x^+. In each decay mode the observed mass distribution is plotted for different x_p intervals. The size of the Λ_c^+ signal in each interval is obtained by fitting the observed mass distribution with the sum of a Gaussian and a low-order polynomial background. The width of the Gaussian is chosen according to the Monte Carlo prediction and the mass is fixed at the fitted value obtained using the sample in the range $0.5 < x_p < 1.0$. The reconstruction efficiencies for the Λ_c^+ in the different decay modes are calculated using a Monte Carlo simulation of these decays in the CLEO detector. In calculating the reconstruction efficiencies, we have assumed that the Λ_c^+'s are produced unpolarized and decay according to phase space. Intermediate resonances in the final state are neglected. The results for the six different decay modes are presented in Tables II–VII. For each x_p interval, $B\,d\sigma/dx_p$ is the corresponding differential cross section with respect to x_p, multiplied by the branching fraction for that decay mode. The errors are statistical only and do not include the contribution from the errors in the Monte Carlo efficiencies, which are treated as part of the systematic errors. In Table VIII, we also present $B\,d\sigma/dx^+$, the differential cross sections with respect to the light-cone variable x^+, since this is the variable used in the derivation of the Bowler and Lund fragmentation functions considered in the next section. This is done for only the three statistically significant decay modes $pK^-\pi^+$, $p\bar{K}^0$, and $\Lambda\pi^+\pi^-\pi^+$.

V. FITS TO THE ANALYTICAL FUNCTIONS

The hadronization process by which charm quarks fragment into charmed mesons and baryons is a QCD process, which, at our center-of-mass energies, is dominated by nonperturbative interactions. The process may be described as $Q \rightarrow h + q$ where Q is the heavy quark, q is a light quark, and h is the hadron. Phenomenological and semiphenomenological attempts at describing the hadronization process are embodied in the calculation of the fragmentation function $D_Q^h(x_p)$, the probability that a quark Q will produce a hadron h with fraction x_p of the quark's original momentum.

Peterson *et al.*[13] have suggested the following form of the fragmentation function:

$$D_Q^h(x_p) = N\left[x_p\left[1-\frac{1}{x_p}-\frac{\epsilon_Q}{1-x_p}\right]^2\right]^{-1},$$

TABLE VI. Inclusive production of Λ_c^+ in the decay mode $\Lambda\pi^+\pi^-\pi^+$.

x_p	Efficiency	Yield	Corrected yield	$B(d\sigma/dx_p)$ (pb)
0.0–0.2	0.067±0.013	5±8	75±120	4±6
0.2–0.3	0.075±0.010	12±11	160±148	16±15
0.3–0.4	0.077±0.010	6±10	78±130	8±13
0.4–0.5	0.078±0.009	12±9	154±117	15±12
0.5–0.6	0.137±0.013	83±26	606±198	14±5
0.6–0.7	0.140±0.015	112±22	800±179	19±4
0.7–0.8	0.151±0.017	70±17	464±124	11±3
0.8–0.9	0.161±0.021	10±11	62±69	1±2
0.9–1.0	0.165±0.050	14±12	85±77	2±2
0.5–1.0		289±41	2017±311	

TABLE VII. Inclusive production of Λ_c^+ in the decay mode $\Xi^- K^+ \pi^+$.

x_p	Efficiency	Yield	Corrected yield	$B(d\sigma/dx_p)$ (pb)
0.5–0.6	0.067±0.011	9±4	134±64	3±1
0.6–0.7	0.065±0.009	16±5	246±84	6±2
0.7–1.0	0.081±0.008	6±3	74±38	1±1
0.5–1.0		31±7	454±112	

where N is a normalization factor and $\epsilon_Q = m_q^2/m_Q^2$. The parameters m_Q and m_q are the masses of the heavy and light quarks, respectively. The Peterson function was intended to describe the fragmentation into mesons as originally proposed, but if the fragmentation into baryons is treated as $Q \to h + \overline{qq}$, where a diquark-antidiquark pair is created from the sea, the original form of the Peterson function remains valid. However, ϵ_Q should now be interpreted as (m_{qq}^2/m_Q^2), where m_{qq} is the mass of the diquark.

Collins and Spiller[14] have argued that Peterson's formula, which behaves as $(1-x_p)^2$ for $x_p \to 1$, disagrees with the reciprocity rule, which states that for $x_p \to 1$, the fragmentation function of the heavy quark into a hadron should equal the structure function of the quark in that hadron. The Collins form of the fragmentation function is

$$D_Q^h(x_p) = N \left[\frac{1-x_p}{x_p} + \frac{2-x_P}{1-x_p}\epsilon'_Q \right](1+x_p^2) \times \left[1 - \frac{1}{x_p} - \frac{\epsilon'_Q}{1-x_p} \right]^{-2},$$

where N is a normalization factor and $\epsilon'_Q = \langle k_T^2 \rangle / m_Q^2$ and $\langle k_T^2 \rangle = 0.45$ GeV^2 with k_T being the transverse hadron momentum.

On the other hand, assuming that the probability P of breaking the color string by creating a quark-antiquark pair is constant per unit time and unit length, Bowler[15] suggests the following form for the fragmentation function:

$$D_Q^h(x^+) = N \frac{(1-x^+)^\beta}{x^+} \exp\left\{ -Bm_Q^2 \left[\frac{M_T^2}{m_Q^2 x^+} - 1 - \ln\left[\frac{M_T^2}{m_Q^2 x^+} \right] \right] \right\},$$

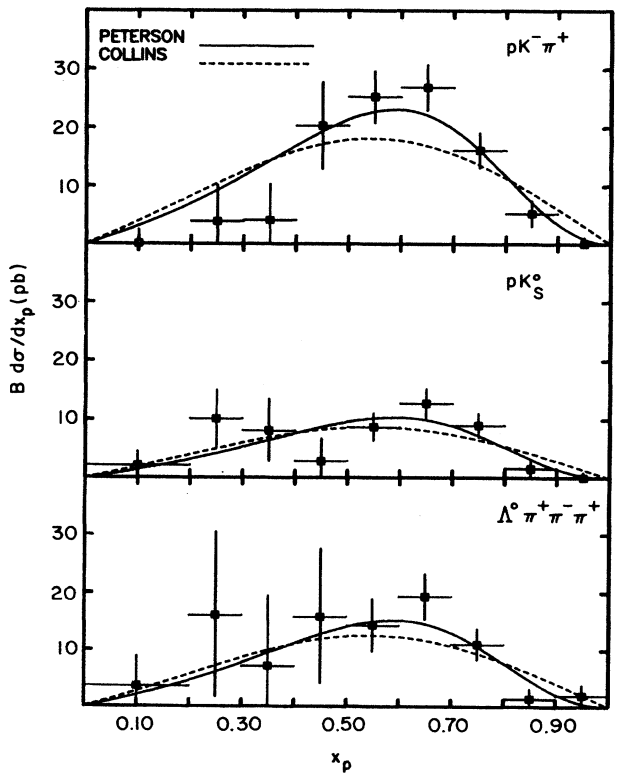

FIG. 8. $B\,d\sigma/dx_p$ distributions for $\Lambda_c^+ \to pK^-\pi^+$, pK_S^0, and $\Lambda\pi^+\pi^-\pi^+$, respectively. The smooth curves are the result of a simultaneous fit to the Peterson (solid lines) and Collins (dashed lines) functions, respectively.

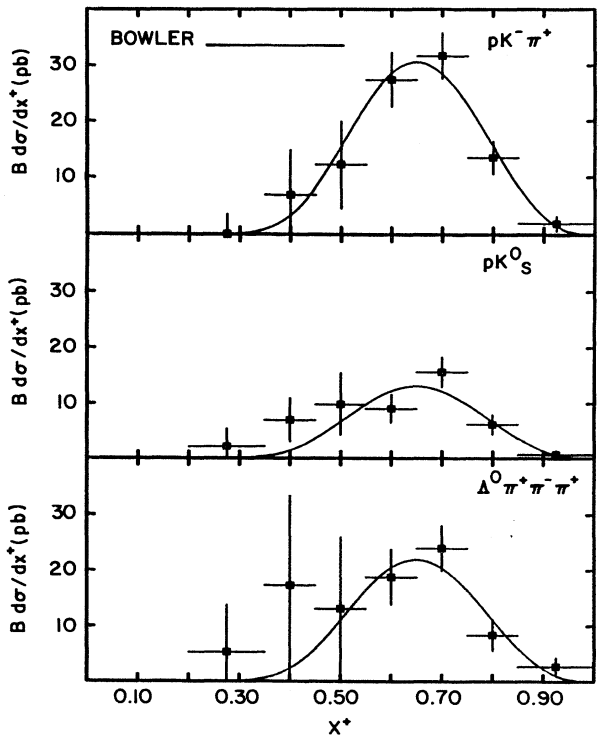

FIG. 9. $B\,d\sigma/dx^+$ distributions for $\Lambda_c^+ \to pK^-\pi^+$, pK_S^0, and $\Lambda\pi^+\pi^-\pi^+$, respectively. The smooth curves are the result of a simultaneous fit to the Bowler function.

TABLE VIII. $B(d\sigma/dx^+)$ (pb).

x^+	$pK^-\pi^+$	$p\bar{K}^0$	$\Lambda\pi^+\pi^-\pi^+$
0.20–0.35	0.0±3.5	2.1±3.2	5.2±8.4
0.35–0.45	6.9±7.8	6.9±4.0	17.3±16.0
0.45–0.55	12.2±7.7	9.8±5.6	13.1±12.0
0.55–0.65	27.4±4.9	9.0±2.6	18.8±5.0
0.65–0.75	31.7±4.1	15.6±2.7	24.0±4.0
0.75–0.85	13.4±2.9	6.1±1.8	8.4±3.0
0.85–1.0	1.9±1.3	0.7±0.7	2.7±1.6

where $M_T=\sqrt{M_h^2+\langle p_T^2\rangle}$ is the transverse mass of the hadron. β is expected to be close to 1. B is a parameter to be determined from fits to data and is related to P by $B=P/(2\kappa^2)$, where κ is the string energy per unit length. It should be noted that the Bowler function is very similar to the Lund symmetric function, which is used in the Lund Monte Carlo simulation.[16]

The analytical representation of the fragmentation distributions do not account for the feed down from higher-spin charmed-baryon states and, to a large extent, disregard QCD and QED radiative corrections. When a fragmentation function is used in the context of a Monte Carlo simulation that takes into account these effects, the function's best-fit parameters turn out to be substantially different from those obtained by direct fitting of the analytical fragmentation function to the experimental fragmentation distribution.[9] However, for the sake of comparison with previous publications we report the results of the direct fitting procedure as discussed below.

We have fitted these analytical fragmentation functions to the data presented in Tables II, III, VI, and VIII. The statistical errors on the Λ_c^+ x_p distributions in the decay modes $p\bar{K}^0\pi^-\pi^+$, $\Lambda\pi^+$, and $\Xi^-K^+\pi^+$ are too large to add significant information to our fragmentation studies. The fitting of the analytical fragmentation functions to the three different inclusive cross-section distributions is performed simultaneously so that all the parameters of the function except the area are constrained to have the same value for the fits to the three different distributions. In Fig. 8, we show the results of the fits to the Peterson and Collins fragmentation functions, while in Fig. 9 we show the result of the fit to the Bowler function. The Bowler function has five different parameters of which we fix two. To calculate the transverse hadron mass, the mass of the hadron M_h is fixed at 2.285 GeV/c^2, the fitted mass of the Λ_c^+, and the average transverse momentum of the hadron is taken as 0.3 GeV/c. The mass of the charm quark m_Q is fixed at 1.5 GeV/c^2. The fit is not very sensitive to values of m_Q between 1.0 to 2.0. The fitted values of the parameters and the quality factor of the fits are presented in Table IX. Also presented in Table IX are the results of corresponding fits to the same functions for the D^{*+} fragmentation distributions measured previously by this experiment.[9]

When the radiative corrections are not applied to the models, the Collins function fails to describe our data, whereas the Peterson and Bowler functions do. The results of the fits could be different if these corrections were applied. The measured value of the fragmentation parameter for the Peterson function ϵ_Q is 0.29±0.05 from the simultaneous fit, which is to be compared with the corresponding ARGUS measurement[4] of $0.23^{+0.07}_{-0.05}$. The value for ϵ_Q obtained from the study of the x_p spectrum of D^{*+}'s is 0.156±0.015 as reported by CLEO.[9] The value of ϵ_Q for charmed baryons is expected to be larger than that for charmed mesons since the mass of the diquark should be higher than that of the quark. The measured values of ϵ_Q are consistent with this expectation.

VI. CROSS SECTIONS AND BRANCHING FRACTIONS

In this section, we present all experimental results such as production cross sections, and relative and absolute branching fractions.

A. Total cross sections

For the decay mode $pK^-\pi^+$, we obtain the total inclusive $B\sigma$ by integrating the measured cross section for all x_p. For the other decay modes, the signals for $x_p<0.5$ are dominated by large errors; so we use the measured inclusive cross sections with $x_p>0.5$ and multiply by an extrapolation factor of 1.44±0.22, calculated by averaging the extrapolation of the Peterson and Bowler functions fitted to the $pK^-\pi^+$ data. The error in the extrapolation factor reflects the errors in the fitted parameters for these functions. This error is added to the other systematic errors which are dominated mainly by the uncertainty in

TABLE IX. Values of fitted parameters for fragmentation functions.

Parameter	Λ_c^+ Simultaneous fit	χ^2/N_{DF}	D^{*+} (Ref. 9) Fit	χ^2/N_{DF}
		Peterson function		
ϵ_Q	0.29±0.05	23/23	0.156±0.015	40/10
		Collins Function		
ϵ'_Q	1.19±0.44	54/23	0.64±0.14	6/10
		Bowler Function		
β	2.86±0.52	12/16	0.95±0.11	8/8
B	1.06±0.23		0.63±0.11	

TABLE X. Measurements of Λ_c^+ inclusive $B\sigma$ and comparison with ARGUS (Ref. 4).

Decay mode	Experiment	$B\sigma(x_p>0.5)$ (pb)	$B\sigma(x_p>0.0)$ (pb)
$pK^-\pi^+$	CLEO	7.2±0.7±1.1	10.0±1.5±1.5
	ARGUS		9.0±1.2±1.0
$p\bar{K}^0$	CLEO	3.2±0.4±0.3	4.6±0.6±0.8
$p\bar{K}^0\pi^-\pi^+$	CLEO	3.1±0.9±0.6	4.5±1.3±1.1
$\Lambda\pi^+$	CLEO	1.3±0.2±0.1	1.9±0.3±0.3
$\Lambda\pi^+\pi^-\pi^+$	CLEO	4.7±0.7±0.5	6.8±1.0±1.3
$\Xi^-K^+\pi^+$	CLEO	1.1±0.3±0.2	1.6±0.4±0.3

our knowledge of the particle identification efficiencies and the Monte Carlo widths of the signals. In Table X, the measured $B\sigma$ corresponding to the six different decay modes are presented for both $x_p>0.5$ and for all x_p.

B. Relative branching fractions

At our center-of-mass energies there is no model-independent way to calculate the absolute branching fractions since we do not know the total cross section for Λ_c^+ production. Since some of the systematic errors are common among the different decay modes, they are partially canceled in the calculation of the relative branching fractions. The signal for the Λ_c^+ has been observed with the highest statistical significance in the $pK^-\pi^+$ decay mode, so the branching fractions of the other decay modes are calculated relative to this mode. The measured cross sections for $x_p>0.5$, as shown in Table X, have been used by CLEO in calculating the relative branching fractions as presented in Table XI. The first error is statistical while the second error is systematic. Comparison with results from ARGUS[4] and E691[5] are also included. We have not included the results from ACCMOR[17] since their results are statistically weak and the Λ_c^+ mass is shifted to higher values. Adding the statistical and systematic errors in quadrature and calculating the weighted average of the three independent measurements, we obtain the latest value of the relative branching fractions as presented in the last column of the table. Our relative ratio between the Λ_c^+ decay branching ratio to $p\bar{K}^0\pi^+\pi^-$ and to $\Lambda\pi^+\pi^-\pi^+$, 0.66±0.22±0.14, is in strong disagreement with the Dubna result[18] of 4.3±1.2. For this reason, we have not included the Dubna results in calculating the weighted averages in Table XI.

C. Absolute branching fractions

From measurements of inclusive baryon production and the study of baryon-lepton and baryon-baryon correlations in B-meson decays, and using the assumption that all baryons in B-meson decays are produced from or in association with charmed baryons, both CLEO[19] and ARGUS[4] have estimated the inclusive branching fraction $B(B\to\Lambda_c^+X)$. Both[20,21] have also reported direct evidence for the inclusive decay $B\to\Lambda_c^+X$ with $\Lambda_c^+\to pK^-\pi^+$. Combining these two measurements, an estimate of the absolute branching fraction $B(\Lambda_c^+\to pK^-\pi^+)$ can be obtained. The measurement of $B(\Lambda_c^+\to pK^-\pi^+)$ from CLEO[22] is (4.3±1.0±0.8)%, which may be stated as (4.3±1.3)% if the statistical and systematic errors are added in quadrature. The corresponding measurement from ARGUS[23] is (4.1±2.4)%, where the error already includes the statistical and systematic contributions. Their weighted average is $B(\Lambda_c^+\to pK^-\pi^+)=(4.3\pm1.1)\%$. Using this estimate of the absolute branching fraction $B(\Lambda_c^+\to pK^-\pi^+)$ and the average relative branching fractions given in Table XI, we obtain an estimate of the absolute branching fractions of the Λ_c^+ into the five other decay modes. We present these results in Table XII for the convenience of the readers. The error includes contributions from the statistical and systematic errors in the measurement of the relative branching fraction and the error in the measurement of $B(\Lambda_c^+\to pK^-\pi^+)$. There have been several attempts to estimate Λ_c^+ absolute branching ratios, reviewed and augmented by Klein[24] and, in part, summarized in the 1990 Particle Data Group compilation.[12] Our results are consistent with the world averages for all decay modes except the $p\bar{K}^0\pi^-\pi^+$, where the world value has a large error.

TABLE XI. Measurements of Λ_c^+ branching fractions relative to that into $pK^-\pi^+$. The last column is the weighted averages with statistical and systematic error combined in quadrature.

Decay mode	ARGUS (Ref. 4)	E691 (Ref. 5)	CLEO '90	Average
$p\bar{K}^0$	0.62±0.15±0.03	0.55±0.17±0.14	0.44±0.07±0.05	0.49±0.07
$p\bar{K}^0\pi^-\pi^+$	1.00±0.3±0.3	<1.7 (90% C.L.)	0.43±0.12±0.04	0.48±0.12
$\Lambda\pi^+$	0.21±0.05±0.04	<0.33 (90% C.L.)	0.18±0.03±0.03	0.19±0.04
$\Lambda\pi^+\pi^-\pi^+$	0.61±0.16±0.04	0.82±0.29±0.27	0.65±0.11±0.12	0.65±0.11
$\Xi^-K^+\pi^+$			0.15±0.04±0.03	0.15±0.04

TABLE XII. Comparison of Λ_c^+ absolute branching fractions (%).

Decay mode	Particle Data Group (Ref. 12)	New
$pK^-\pi^+$	2.8±0.8	4.3±1.1
$p\bar{K}^0$	1.6±0.6	2.1±0.6
$p\bar{K}^0\pi^-\pi^+$	8.1±3.5	1.8±0.6
$\Lambda\pi^+$		0.8±0.3
$\Lambda\pi^+\pi^-\pi^+$	1.9±0.7	2.8±0.9
$\Xi^-K^+\pi^+$		0.6±0.2
Total measured		12.4±1.7

D. Comparison with theoretical models

Most of the theoretical efforts to understand charm decays have been devoted to charmed-meson studies.[25] For charmed baryons, with the exception of early phase-space-based estimates of relative decay branching ratios by Lee, Quigg, and Rosner,[26] only the decay rates into two-body and quasi-two-body final states have been studied theoretically. Because of resonance decay, some of the latter studies apply, in part, to multibody final states. The statistical model by Lee, Quigg, and Rosner[26] predicts $B(\Lambda_c^+\to\Lambda\pi^+)/B(\Lambda_c^+\to\Lambda\pi^+\pi^-\pi^+)=0.75$, in disagreement with our result 0.28±0.07, while it agrees with our ratio $B(\Lambda_c^+\to p\bar{K}^0)/B(\Lambda_c^+\to p\bar{K}^0\pi^+\pi^-)=1.0\pm0.3$. We compare our experimental measurements of the two-body decay modes $\Lambda\pi^+$ and $p\bar{K}^0$ with some of the theoretical models which are briefly described below. Korner, Kramer, and Willrodt[27] (KKW) have calculated these decay rates in a naive quark model using wave functions based on U(2,2). They have also calculated them using an SU(4) model and a current-algebra (CA) model. Hussain and Scadron[28] (HS) have used current-algebra and nonrelativistic SU(6) wave functions. In their model, the quark interaction is spin and SU(3)-flavor independent and orbital contributions to the magnetic moments have been ignored. Calculations done by Pakvasa, Rosen, Tuan, and Division[29] (PRTD) are also based on current algebra and the factorization approximation as the HS model, but they have employed flavor-SU(3) selection rules to express the amplitudes for individual decay modes in terms of a set of invariant amplitudes. Ebert and Kallies[30] (EK) have done their calculation by employing the QCD-corrected weak Hamiltonian and wave functions of the heavy-quark bag model; baryon matrix elements of the parity-violating part of the charm-changing weak Hamiltonian were also included. Guberina, Tadic, and Trampetic[31] (GTT) used a similar approach to KKW but they also take account of soft-gluonic contributions. In Table XIII, we present a comparison of our measurements with the above theoretical models. The partial widths to the $\Lambda\pi^+$ and $p\bar{K}^0$ decay modes are calculated using the estimated absolute branching fractions in Table XII and the Λ_c^+ lifetime of $(1.79^{+0.23}_{-0.17})\times10^{-13}$ seconds.[12] We do not use the above partial widths to calculate the ratio of the partial widths, since they have large systematic errors associated with them. Instead, we calculate the ratio of the partial widths $\Gamma(\Lambda\pi^+)/\Gamma(p\bar{K}^0)$ by using the direct CLEO measurements of the inclusive $B\sigma$ for $x_p>0.5$ reported in Table X. In this way, we get $\Gamma(\Lambda\pi^+)/\Gamma(p\bar{K}^0)=(0.41\pm0.09)$. The error quoted includes both the statistical and systematic contributions. From a comparison of the spectator decay diagrams for $\Lambda_c^+\to\Lambda\pi^+$ to that for $\Lambda_c^+\to p\bar{K}^0$, one would naively expect the latter to be suppressed by a factor of 9 relative to the former due to color mismatching, which is quite different from the measured value above. However, it must be pointed out that this naive expectation is not reflected in more detailed theoretical calculations and has also not been observed in the case of charmed-meson decays. The branching fractions for the D^0 color suppressed and allowed decays are $B(D^0\to\bar{K}^0\pi^0)=(2.7\pm1.2)\%$ and $B(D^0\to K^-\pi^+)=(3.71\pm0.25)\%$, respectively.[12]

VII. CONCLUSIONS

In conclusion, we have measured the branching fraction of the Λ_c^+ into five different decay modes relative to that into $pK^-\pi^+$. Our measurements are an improvement over the earlier Mark II[1] results and also consistent with recent ARGUS[4] and E691[5] results as shown in Table XI. The branching fractions for decays into two-body final states have been compared with theoretical expectations; they strongly disagree with two of the models. Furthermore, color suppression does not seem to play a significant role, as suggested by results on D^0 decay.

Our measurement of the fragmentation distribution for Λ_c^+ production in e^+e^- annihilation is also a considerable improvement relative to our previous measurement. We have compared these distributions with the theoreti-

TABLE XIII. Comparison of Γ between theory and experiment (Γ in units of 10^{11} sec^{-1}).

	Model							
Γ	Quark	KKW[a] SU(4)	CA	HS[b]	PRTD[c]	EK[d]	GTT[e]	Experiment
$\Lambda\pi^+$	0.8	0.28	0.38	0.77	1.0	0.32		0.39±0.17
$p\bar{K}^0$	8.9	0.63	0.16	1.64	2.78	0.17		1.17±0.42
$\Gamma(\Lambda\pi^+)/\Gamma(p\bar{K}^0)$	0.09	0.44	2.4	0.47	0.36	1.88	0.85	0.41±0.09

[a]Reference 27.
[b]Reference 28.
[c]Reference 29.
[d]Reference 30.
[e]Reference 31.

cal models. The Peterson, Bowler, and Lund symmetric functions provide a good parametrization of our results, while the Collins function does not.

ACKNOWLEDGMENTS

We gratefully acknowledge the effort of the CESR staff. P.S.D. thanks the Presidential Young Investigator program of the NSF, and A.P. thanks the A.P. Sloan Foundation for support. This work was supported by the National Science Foundation and the U.S. Dept. of Energy under Contract Nos. DE-AC0276ER01428, DE-AC0276ER03064, DE-AC0276ER01545, DE-AC0278ER05001, DE-AC0283ER40103, and DE-FG05-86ER40272. The supercomputing resources of the Cornell Theory Center were used in this research.

[1]Mark II Collaboration, G. S. Abrams *et al.*, Phys. Rev. Lett. **44**, 10 (1980).

[2]CLEO Collaboration, T. S. Bowcock *et al.*, Phys. Rev. Lett. **55**, 9 (1985).

[3]ARGUS Collaboration, in *Hadrons, Quarks and Gluons,* Proceedings of the XXIInd Rencontre de Moriond, Les Arcs, France, 1987, edited by J. Tran Thanh Van (Editions Frontieres, Gif-sur-Yvette, 1987).

[4]ARGUS Collaboration, H. Albrecht *et al.*, Phys. Lett. B **207**, 109 (1988); M. Danilov, in *Proceedings of the XXIV International Conference on High Energy Physics,* Munich, West Germany, 1988, edited by R. Kotthaus and J. Kuhn (Springer, Berlin, 1988).

[5]J. C. Anjos *et al.*, Phys. Rev. D **41**, 801 (1990).

[6]Mark II Collaboration, J. M. Yelton *et al.*, Phys. Rev. Lett. **49**, 430 (1982); HRS Collaboration, M. Derrick *et al.*, *ibid.* **53**, 1971 (1984); DELCO Collaboration, H. Yamamoto *et al.*, *ibid.* **54**, 522 (1985); HRS Collaboration, M. Derrick *et al.*, Phys. Lett. **146B**, 261 (1984); TPC/Two γ Collaboration, H. Aihara *et al.*, Phys. Rev. D **34**, 1945 (1986); HRS Collaboration, S. Abachi *et al.*, in *Proceedings of the XXIII International Conference on High Energy Physics,* Berkeley, California, 1986, edited by S. C. Loken (World Scientific, Singapore, 1987).

[7]TASSO Collaboration, M. Althoff *et al.*, Phys. Lett. **126B**, 493 (1983); **136B**, 139 (1984); JADE Collaboration, W. Bartel *et al.*, *ibid.* **146B**, 121 (1984); **161B**, 197 (1985).

[8]ARGUS Collaboration, H. Albrecht *et al.*, Phys. Lett. **150B**, 235 (1985); **153B**, 343 (1985); ARGUS Collaboration, H. Albrecht *et al.*, in *Proceedings of the XXIII International Conference on High Energy Physics,* (Ref. 6); ARGUS Collaboration, R. S. Orr, in *Proceedings of the International Europhysics Conference on High Energy Physics,* Bari, Italy, 1985, edited by L. Nitti and G. Preparata (Laterza, Bari, 1985), p. 517.

[9]CLEO Collaboration, C. Bebek *et al.*, Phys. Rev. Lett. **49**, 610 (1982); CLEO Collaboration, P. Avery *et al.*, *ibid.* **51**, 1139 (1983); CLEO Collaboration, A. Chen *et al.*, *ibid.* **51**, 634 (1983); CLEO Collaboration, D. Bortoletto *et al.*, Phys. Rev. D **37**, 1719 (1988); **39**, 1471(E) (1989).

[10]We use the scaling variables x_p and x^+ rather than the momentum of the Λ_c^+ throughout this paper.

[11]CLEO Collaboration, D. Andrews *et al.*, Nucl. Instrum. Methods **211**, 47 (1983); CLEO Collaboration, S. Behrends *et al.*, Phys. Rev. D **31**, 2161 (1985).

[12]Particle Data Group, J. J. Hernández *et al.*, Phys. Lett. B **239**, 1 (1990).

[13]C. Peterson *et al.*, Phys. Rev. D **27**, 105 (1983).

[14]P. Collins and T. Spiller, J. Phys. G **11**, 1289 (1985).

[15]M. G. Bowler, Z. Phys. C **11**, 169 (1981); **22**, 155 (1984).

[16]B. Andersson *et al.*, Phys. Rep. **91**, 33 (1983).

[17]Amsterdam - Bristol - CERN - Cracow - Munich - Rutherford (ACCMOR) Collaboration, S. Barlag *et al.*, Z. Phys. C **48**, 29 (1990).

[18]A. N. Aleev *et al.*, Z. Phys. C **23**, 333 (1984).

[19]CLEO Collaboration, M. S. Alam *et al.*, Phys. Rev. Lett. **59**, 22 (1987); CLEO Collaboration, Yuichi Kubota, *Proceedings of the International Conference on Heavy Quark Physics,* edited by P. S. Drell and D. L. Rubin (AIP, New York, 1989), p. 142.

[20]CLEO Collaboration, M. S. Alam *et al.*, presented at the International Symposium on Photon and Lepton Physics, Munich, Federal Republic of Germany, 1988 (unpublished).

[21]ARGUS Collaboration, H. Albrecht *et al.*, Phys. Lett. B **210**, 263 (1988).

[22]CLEO Collaboration, M. S. Alam *et al.*, CLEO Internal Memo CBX 90-39, 1990 (unpublished). In this memo, $B(\Lambda_c^+ \to pK^-\pi^+) = (4.4 \pm 1.2^{+1.2}_{-1.0})\%$ was quoted as a preliminary value. A more recent value is $(4.3 \pm 1.0 \pm 0.8)\%$, which is still not the final value, as some more checks on device solid angles and detection efficiencies are being investigated.

[23]CLEO Collaboration, Sheldon Stone, in *Weak Interactions and Neutrinos,* proceedings of the XII International Workshop, Ginosar, Israel, 1989, edited by P. Singer and B. Gad Eilam [Nucl. Phys. B (Proc. Suppl.) **13** (1989)]. The ARGUS value of $B(\Lambda_c^+ \to pK^-\pi^+) = (4.4 \pm 2.4)\%$ is quoted from this report.

[24]S. R. Klein, J. Mod. Phys. A **5**, 1457 (1990), and references therein.

[25]M. B. Einhorn and C. Quigg, Phys. Rev. D **12**, 2015 (1975); A. N. Kamal and R. C. Verma, *ibid.* **35**, 3515 (1987); L. L. Chau and H. Y. Cheng, *ibid.* **36**, 137 (1987); M. Bauer, B. Stech, and M. Wirbel, Z. Phys. C **34**, 103 (1987).

[26]B. W. Lee, C. Quigg, and J. L. Rosner, Phys. Rev. D **15**, 157 (1977).

[27]J. G. Korner *et al.*, Z. Phys. C **2**, 117 (1979).

[28]F. Hussain and M. D. Scadron, Il Nuovo Cimento **79A**, 248 (1984).

[29]S. Pakvasa *et al.*, Phys. Rev. D **42**, 3746 (1990).

[30]D. Ebert and W. Kallies, Z. Phys. C **29**, 643 (1985).

[31]B. Guberina, D. Tadic, and J. Trampetic, Z. Phys. C **13**, 251 (1982).